Molecular Therapy
Oncology
Original Article

Targeting MELK improves PD-1 blockade efficiency in cervical cancer via enhancing antitumor immunity

Dongjiao Wang,[1] Fei Zou,[2] Yu Li,[3] Jinqiu Hu,[4] and Ling Gao[3]

[1]Department of Gynecological Oncology, The First Hospital of Jilin University, Changchun 130021, China; [2]Department of Pediatrics, The First Hospital of Jilin University, Changchun 130021, China; [3]Department of Radiation Oncology & Therapy, The First Hospital of Jilin University, Changchun 130021, China; [4]Pathology Teaching and Research Office, Changchun Medical College, Changchun 130021, China

The balance between T helper 1 (Th1) and T helper 2 (Th2) has a critical function in determining intratumoral immune response and anti-PD-1 immunotherapy. The level of maternal embryonic leucine zipper kinase (MELK) is reported to correlate with infiltration of immune cells in cancers, but the underlying molecular mechanism is not clarified. In the present study, we aimed to elucidate the potential function of MELK in cervical cancer. We found that MELK was upregulated and played an oncogenic role in cervical cancer. MELK overexpression shifted Th1/Th2 balance toward Th2 predisposition in mouse cervical tumors *in vivo* and naive T cells from human PBMCs *in vitro*, whereas MELK knockdown exhibited opposite effects. MELK overexpression activated NF-κB signaling and promoted IL-6 secretion by cervical cancer cells. Depletion of IL-6 by neutralization antibodies abrogated the influence of MELK on Th1/Th2 balance. In addition, MELK modulated the antitumor activity of cytotoxic $CD8^+$ T cells in cervical tumors, but depletion of Th2 cells by IL-4 neutralization abrogated this effect. Finally, MELK overexpression conferred tolerance to PD-1 blockade in cervical tumors, whereas targeting MELK by OTSSP167 significantly enhanced PD-1 blockade efficiency. Our data elucidated a novel role of MELK in regulating Th1/Th2 balance and anti-PD-1 immunotherapy in cervical cancer.

INTRODUCTION

Cervical cancer is a frequently occurring gynecologic malignancy. Global cancer statistics indicates that there were an estimated 604,127 new cervical cancer cases and 341,831 cervical cancer related death in 2020, becoming the fourth most common cancer and leading cause of cancer-related death among women worldwide.[1] Human papillomavirus (HPV) infection is a major cause of cervical cancer. HPV DNAs are identified in nearly 95% of malignant cervical lesions.[2] The incidence and death rates of cervical cancer are much higher in low-income countries due to the prevalence of HPV infection. Treatment options for advanced cervical cancer include surgical resection, chemotherapy, and radiation therapy. However, the effect is limited and there is a lack of second-line treatment option. Recently, immunotherapy with checkpoint inhibitors has attracted much attention for cervical cancer treatment. The rationale for using immunotherapy is based on multiple molecular features of cervical cancer, including high mutational burden and microsatellite instability, upregulation of programmed death ligand 1 (PD-L1) expression, and high tumor inflammatory state.[3] Programmed cell death 1 (PD-1) is a co-stimulatory receptor for exhausted T cells during chronic inflammation and cancer development. Its binding partner PD-L1 is highly expressed in 35%–96% of cervical cancers.[4] In 2018, pembrolizumab, a humanized monoclonal anti-PD1 antibody, was approved for the treatment of recurrent and metastatic $PD\text{-}L1^+$ cervical tumors by the US Food and Drug Administration.[5] Nevertheless, the response rate for pembrolizumab is only ∼15%.[5] A better understanding of the immunosuppressive microenvironment and searching for novel targets for combined therapy may improve the therapeutic efficiency of PD-1 blockade in cervical cancer.

Current studies of cancer immunotherapy reveal a critical role for $CD4^+$ T helper (Th) cells in antitumor response by regulating cytotoxic T cell activity directly or indirectly.[6] Th cells can be protumorigenic or antitumorigenic, which further contributes to the complexity of the tumor microenvironment. Th1 and Th2 are two major subsets of Th cells. Th1 cells are involved in the immune response against intracellular viral or bacterial pathogens, whereas Th2 cells take part in the immune response to extracellular pathogens and allergic reactions. Generation of Th1 cells is dependent on interferon-γ (IFN-γ) and interleukin-12 (IL-12) cytokines, activation of signal transducer and activator of transcription 1 (STAT1) and STAT4 signaling and induction of expression of transcription factor T-bet.[7] In comparison, polarization to Th2 cells is dependent on IL-4 production, activation of STAT6 signaling, and upregulation of GATA3 transcription factor.[7] Th1 differentiation is suppressed by IL-4, whereas Th2 differentiation is restrained by IFN-γ; thus, the balance between IL-4 and IFN-γ feedback loops is vital for the balancing act

Received 23 May 2023; accepted 5 January 2024;
https://doi.org/10.1016/j.omton.2024.200759.

Correspondence: Ling Gao, Department of Radiation Oncology & Therapy, The First Hospital of Jilin University, Changchun 130021, China.
E-mail: linggao@jlu.edu.cn

between Th1 and Th2-mediated immune response.[6] Th1 cells are well characterized for their antitumorigenic function by enhancing the cytotoxicity activity of $CD8^+$ T cells, inhibiting angiogenesis, and inducing antitumorigenic M1 macrophages in tumor.[8,9] In contrast, the role of Th2 in cancer has been viewed as controversial because there is evidence indicating pro- or antitumorigenic roles of Th2 in cancers, which seems to be context dependent.[6] According to Bretscher's Th2-skewing hypothesis, successful antitumor immunity is mediated mostly by Th1 and $CD8^+$ T cells, whereas a bias of Th2 cells is prone to tumor escape.[10] Accumulated evidence in the past decades supports the notion that Th1 and Th2 cells have critical and opposing roles in determining intratumoral immune response.[6] Thus, a shift in Th1/Th2 balance toward a higher ratio of Th1/Th2 may reverse the immunosuppressive tumor microenvironment.

Maternal embryonic leucine zipper kinase (MELK) is a member of the AMP-related serine-threonine kinase family. MELK is involved in intracellular signaling transduction and affects many cellular processes, including cell cycle, proliferation, apoptosis, and posttranscriptional modification.[11] What is more, MELK is proved to promote tumorigenesis and therapeutic resistance in various cancers.[11] MELK is upregulated in cervical cancer, and knockdown of MELK inhibits cell growth and promotes apoptosis of cervical cancer cells.[12,13] Moreover, there is increasing evidence suggesting that MELK is associated with immune cell infiltration. In hepatocellular carcinoma, MELK expression is correlated with the infiltration of B cells, $CD8^+$ T cells, $CD4^+$ T cells, macrophages, neutrophils, and dendritic cells.[14] MELK is also positively correlated with immune checkpoint genes in hepatocellular carcinoma.[14] In addition, MELK expression is demonstrated to correlate with immune cell infiltration in glioma and breast cancer.[15,16] However, the exact role of MELK in immune cell infiltration and the underlying mechanism is not fully understood. In the present study, the potential function of MELK in the cervical microenvironment was evaluated. Our data provided a novel role for MELK in regulating Th1/Th2 balance, antitumor immunity of $CD8^+$ T cells, and PD-1 blockade efficiency in cervical cancer. MELK may be a potential target for cervical cancer treatment.

RESULTS

MELK plays an oncogenic role in cervical cancer

The potential function of MELK in cervical cancer was evaluated in our study. MELK expression was checked. According to the Tumor Immune Estimation Resource (TIMER) database, MELK was significantly upregulated in various cancers (Figure S1A). Data from The Cancer Genome Atlas (TCGA) and the GEO database (GSE6791, GSE52903, and GSE67522) indicated that MELK was significantly overexpressed in cervical cancer patients (Figures S1B and S1C). However, MELK expression exhibited no connection with tumor stages of cervical cancer patients, suggesting that MELK upregulation may be an early event for cervical cancer tumorigenesis (Figure S1D). In addition, MELK expression showed no connection with the overall survival of cervical cancer patients (Figure S1E). In our study, MELK expression in cervical cancer cell lines was evaluated by western blot. Compared with nontumor control, the expression levels of MELK were high in Ca Ski and HeLa cells and low in SiHa and HT-3 cells (Figure 1A). To evaluate the potential function of MELK in cervical cancer, MELK was forced to express in SiHa and HT-3 cells by transducing with MELK expression lentivirus (Figure 1B). Forced MELK expression promoted the cell growth of SiHa and HT-3 cells (Figure 1C). In a soft agar assay, MELK overexpression facilitated anchorage-independent growth of SiHa and HT-3 cells, indicating enhanced malignant transformation of SiHa and HT-3 cells (Figures 1D and 1E). In addition, ectopic MELK expression evidently accelerated the tumor growth of SiHa cells in nude mice (Figures 1F–1H). Next, the potential function of MELK in cervical cancer was evaluated by loss-of-function assays. MELK was knocked down in HeLa cells by introducing short hairpin RNAs specifically targeting MELK (shMELK-1 and shMELK-2) (Figure 1I). MELK knockdown suppressed the growth and soft agar colony formation of HeLa cells (Figures 1J–1L). In a tumor xenograft model, the depletion of MELK evidently inhibited the tumor growth of HeLa cells in nude mice (Figures 1M–1O). Taken together, our results indicated that MELK played an oncogenic role in cervical cancer.

MELK overexpression reprograms the immune microenvironment to favor Th2 predisposition in cervical tumors

Correlation of MELK with immune cell infiltration in cervical cancer was evaluated. According to the TIMER algorithm, MELK expression was associated with the infiltration of B cells, $CD4^+$ T cells, and macrophages in cervical cancer patients (Figure S2A). Next, the Tumor-Immune System Interactions Database (TISIDB) was used to evaluate the connection between MELK expression and infiltrating immune cells. MELK expression was positively correlated with the infiltration of active $CD4^+$ T cells and Th1 cells, and negatively correlated with the infiltration of Th17 cells and macrophages in cervical cancer patients (Figure S2B). Data from TIMER indicated that MELK expression was positively associated with immunoinhibitory molecules, including transforming growth factor-β type 1 receptor (TGFBR1), TGFB1, and PD-1 in cervical cancer patients (Figure S2C). The correlation between MELK expression and immune cell infiltration was evaluated in various cancers. MELK expression was positively correlated with the infiltration of active $CD4^+$ T cells and Th1 cells and negatively correlated with Th2 infiltration in a variety of cancers (Figures S3A and S3B). These data suggested that MELK upregulation may affect Th1/Th2 balance in cancers and favored a Th2 bias to promote tumor escape in antitumor immune responses. To evaluate this, a subcutaneous U14-bearing mice model was built in C57BL/6 mice. U14 is a mouse cervical cancer cell line. MELK was ectopically overexpressed in U14 cells and subcutaneously injected into C57BL/6 mice (Figure 2A). To evaluate the influence of MELK overexpression on the immune microenvironment of cervical tumors, infiltrating immune cells were evaluated by flow cytometry. The gating strategy and representative plots of these infiltrating immune cells are depicted in Figure S4. Our data indicated that ectopic MELK expressing increased the infiltration of regulator T cells (Treg), tumor-associated macrophages (TAM), and myeloid-derived suppressor cells (MDSCs) and suppressed the infiltration of cytotoxic T cells (cyto T) in U14 cervical

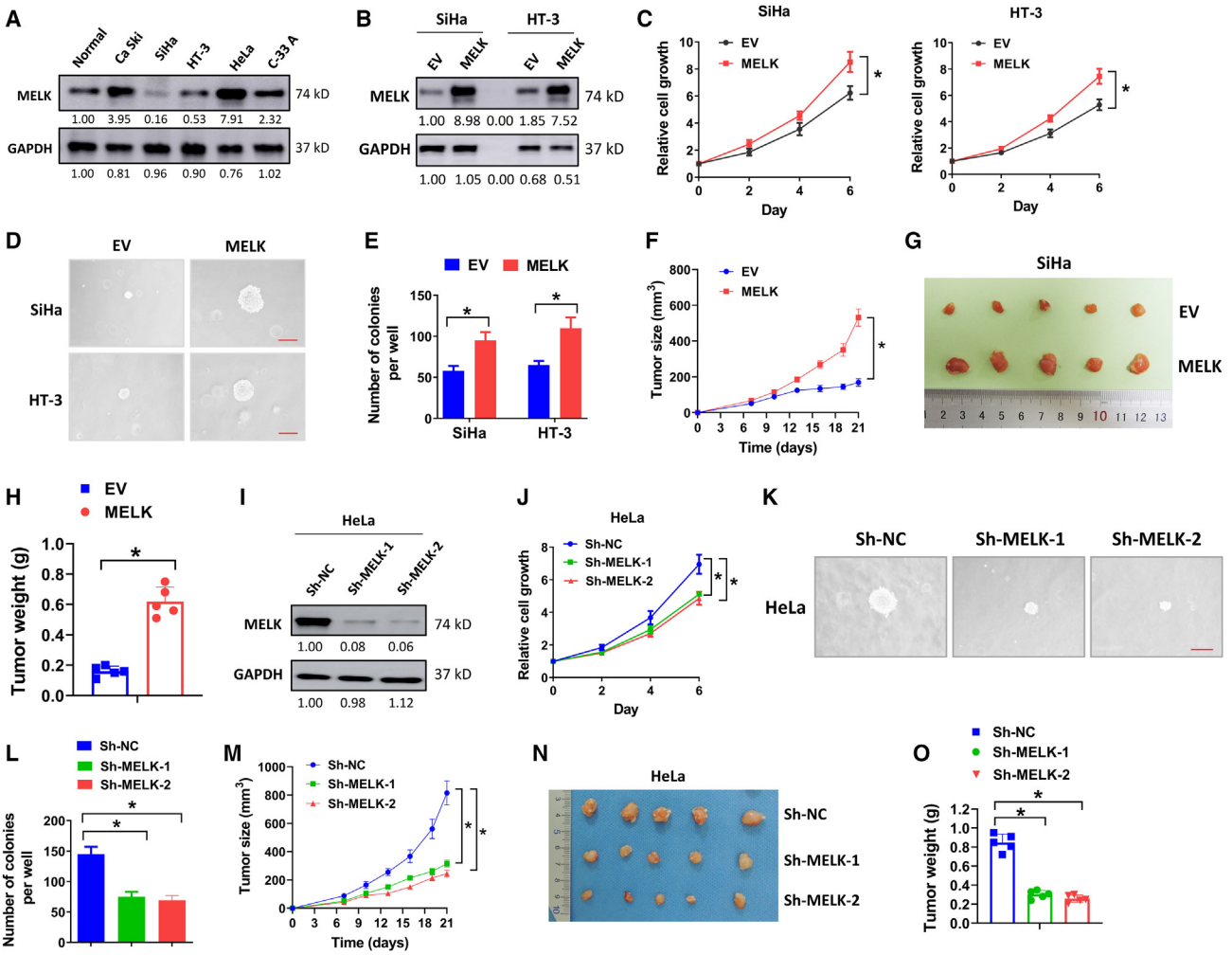

Figure 1. MELK acts an oncogenic role in cervical cancer

(A) MELK expression in cervical cancer cell lines and nontumor normal tissue control were evaluated by western blot. (B) SiHa and HT-3 cells were transduced with MELK expression lentivirus or EV control. Then, MELK expression was evaluated by Western blot. (C) SiHa or HT-3 cells (3,000/well) transduced with MELK expression lentivirus or EV control were seeded in 96-well plates, and cell viability was evaluated at days 0, 2, 4, and 6. (D and E) SiHa or HT-3 cells (5,000/well) transduced with MELK expression lentivirus or EV control were used for soft agar assay. Representative images (D) and number of colonies per well (E) are shown. (F–H) SiHa cells (2×10^6) transduced with MELK expression lentivirus or EV control were subcutaneously injected into nude mice and allowed to grow for 3 weeks. Tumor growth (F), images (G), and weight (H) are shown. (I) HeLa cells were transduced with Sh-NC, shMELK-1, or shMELK-2 lentivirus. Then, MELK expression was evaluated by western blot. (J) HeLa cells (3,000/well) transduced with Sh-NC, shMELK-1, or shMELK-2 were seeded in 96-well plates, and cell viability was evaluated at days 0, 2, 4, and 6. (K and L) HeLa cells (3,000/well) transduced with Sh-NC, shMELK-1, or shMELK-2 were used for soft agar assay. Representative images (K) and number of colonies per well (L) are shown. (M–O) HeLa cells (2×10^6) transduced with Sh-NC, shMELK-1, or shMELK-2 were subcutaneously injected into nude mice and allowed to grow for 3 weeks. Tumor growth (M), images (N), and weight (O) are shown. Data are shown as mean ± SD. *$p < 0.05$.

tumors (Figure 2B). In addition, MELK overexpression showed no influence on the infiltration of $CD4^+IL\text{-}17^+$ Th17 cells in U14 cervical tumors (Figure S5). The immunosuppressive tumor microenvironment was characterized by the upregulation of some effectors, such as PD-L1, TGFB1, IL-10, and IL-13.[17] In our study, MELK overexpression evidently promoted the expression of PD-L1, TGFB1, IL-10, and IL-13 in U14 cervical tumors (Figures 2C and 2D). These data suggested that the upregulation of MELK may foster an immunosuppressive microenvironment in cervical cancer.

Th1 cells were characterized by the expression of IFN-γ, whereas Th2 cells were characterized by the expression of IL-4. In our study, Th1 cells and Th2 cells were defined as $CD3^+CD4^+IFN\text{-}\gamma^+IL4^-$ and $CD3^+CD4^+IFN\text{-}\gamma^-IL4^+$, respectively. Infiltration of Th1 and Th2 cells in U14 cervical tumors was evaluated by flow cytometry. MELK overexpression significantly increased the percentage of Th2 cells and decreased the percentage of Th1 cells in the $CD4^+$ T cell subset of U14 cervical tumors, indicating that MELK overexpression affected Th1/Th2 balance and induced a Th2 predisposition

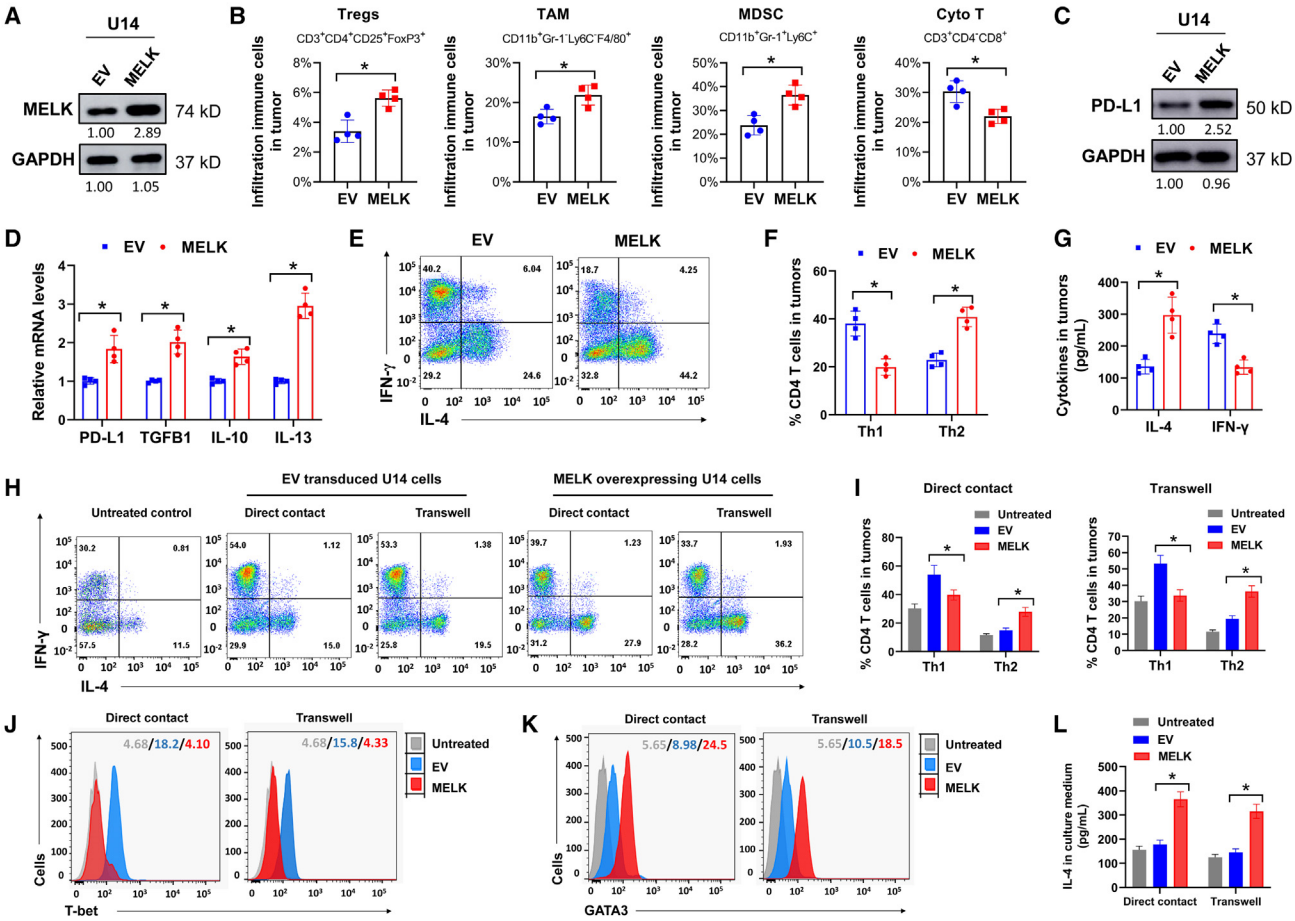

Figure 2. MELK overexpression reprograms the immune microenvironment to favor Th2 predisposition in mouse cervical tumors

(A) U14 cells were transduced with MELK expression lentivirus or EV control, and MELK expression was evaluated by western blot. (B) U14 cells (2×10^6) transduced with MELK expression lentivirus or EV control were subcutaneously injected into C57BL/6 mice for 4 weeks; then, infiltrating Treg, TAM, MDSCs, and Cyto T cells were evaluated by flow cytometry. (C) PD-L1 expression in MELK overexpression U14 cells was evaluated by western blot. (D) Relative expression of PD-L1, TGFB1, IL-10, and IL-13 in MELK or EV introducing U14 tumors were evaluated by quantitative real-time PCR. (E and F) Th1 ($CD3^+CD4^+IFN\text{-}\gamma^+IL4^-$) and Th2 ($CD3^+CD4^+IFN\text{-}\gamma^-IL4^+$) cells in MELK or EV expressing U14 tumors were evaluated by flow cytometry. Representative plots (E) and percentages of Th1 and Th2 cells (F) in $CD4^+$ T cells are shown. (G) IL-4 and IFN-γ production in MELK or EV expressing U14 tumors were evaluated by ELISA. (H–L) Naive T cells isolated from healthy C57BL/6 mice were activated by anti-CD3 and anti-CD28 antibodies, then cocultured with EV transduced or MELK expressing U14 cells by direct contact or indirectly through transwell system. Th1 ($CD3^+CD4^+IFN\text{-}\gamma^+IL4^-$) and Th2 ($CD3^+CD4^+IFN\text{-}\gamma^-IL4^+$) cells were evaluated by flow cytometry. Representative plots (H) and percentages of Th1 and Th2 cells (I) in $CD4^+$ T cell subset are shown. Representative histogram of T-bet^+ (J) or $GATA3^+$ (K) T cells were shown. IL-4 expression in culture medium was evaluated by ELISA assay (L). Data are shown as mean ± SD. *$p < 0.05$.

(Figures 2E and 2F). The levels of Th1-related cytokine IFN-γ and Th2-related cytokine IL-4 were evaluated by ELISA assay. MELK overexpression obviously increased the level of IL-4 and decreased the level of IFN-γ in U14 cervical tumors (Figure 2G). Naive T cells can be activated and differentiated into Th1 or Th2 cells based on the cytokine milieu.[6] In our study, Naive T cells isolated from healthy C57BL/6 mice were activated by anti-CD3 and anti-CD28 antibodies, then were co-cultured with U14 cells by direct contact or indirectly through transwell system. Compared with untreated controls, T cells cocultured with empty vector (EV) transduced U14 cells directly or indirectly showed increased polarization of Th1 and Th2 cells (Figures 2H and 2I). In comparison, T cells cocultured with MELK overexpressing U14 cells directly or indirectly showed a shift in Th1/Th2 balance toward Th2 predisposition (Figures 2H and 2I). T-bet and GATA3 were lineage-specific transcription factors for Th1 and Th2, respectively. In our study, the percentage of T-bet^+ T cells was increased by coculturing with EV-transduced U14 cells compared with untreated control, and this effect was diminished in T cells cocultured with MELK overexpressing U14 cells (Figures 2J and 2K). In contrast, the percentage of $GATA3^+$ T cells was increased by coculturing with EV transduced U14 cells compared with untreated control, and further strengthened in T cells cocultured with MELK overexpressing U14 cells (Figures 2J and 2K). The levels of IL-4 in culture medium of these cells were evaluated

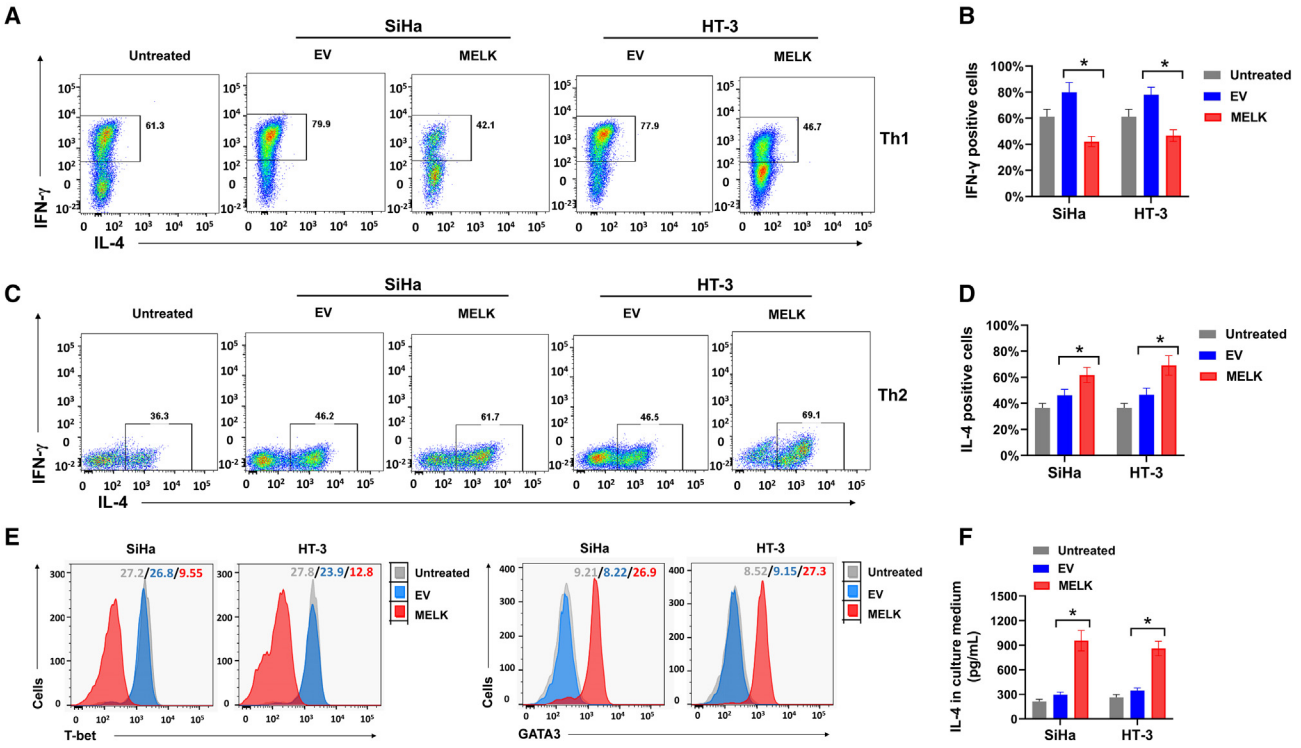

Figure 3. MELK overexpression promotes Th2 polarization and inhibits Th1 polarization of active CD4$^+$ T cells from human PBMCs

(A and B) Naive T cells from human PBMCs were cocultured with EV or MELK transduced SiHa and HT-3 cells indirectly through transwell system under Th1 polarizing conditions. Representative plots (A) and percentages of IFN-γ$^+$IL-4$^-$ Th1 cells (B) are shown. (C–F) Naive T cells from human PBMCs were cocultured with EV or MELK transduced SiHa and HT-3 cells indirectly through transwell system under Th2 polarizing conditions. Representative plots (C) and percentages of IFN-γ$^-$IL-4$^+$ Th2 cells (D) are shown. Representative histogram of T-bet$^+$ or GATA3$^+$ T cells are displayed (E). IL-4 production in culture medium was evaluated by ELISA assay (F). Data are shown as mean ± SD. *p < 0.05.

by ELISA assay. T cells co-cultured with MELK overexpressing U14 cells directly or indirectly showed elevated production of IL-4 compared with untreated T cells or T cells co-cultured with EV transduced U14 cells (Figure 2L). These data indicated that MELK overexpression shifted Th1/Th2 balance toward Th2 skewed in mouse cervical tumors.

This is also tested in human T cells. Naive T cells were isolated from human peripheral blood mononuclear cells (PBMCs) and activated by anti-CD3 and anti-CD28 antibodies, and then cocultured with SiHa and HT-3 cells indirectly through transwell system under Th1 or Th2 polarizing conditions. Under Th1 polarizing conditions, T cells cocultured with MELK overexpressing SiHa or HT-3 cells showed reduced percentages of IFN-γ$^+$IL-4$^-$ Th1 cells compared with T cells cocultured with EV-transduced SiHa or HT-3 cells (Figures 3A and 3B). Under Th2 polarizing conditions, the percentage of IFN-γ$^-$IL-4$^+$ Th2 cells was increased by coculturing with EV-transduced SiHa or HT-3 cells, and this was further enhanced by MELK overexpression in these cells (Figures 3C and 3D). These results indicated that MELK overexpression promoted Th2 polarization and inhibited Th1 polarization. Meanwhile, MELK overexpression increased the percentages of GATA3$^+$ T cells and decreased the percentages of T-bet$^+$ cells under Th2 polarizing conditions, respectively (Figure 3E). In addition, T cells cocultured with MELK overexpressing SiHa or HT-3 cells showed increased production of IL-4 compared with T cells cocultured with EV-transduced cells under Th2 polarizing conditions (Figure 3F). Above all, our results indicated that MELK overexpression inhibited Th1 polarization and promoted Th2 polarization in U14 cervical tumors *in vivo* and active CD4$^+$ T cells from human PBMCs *in vitro*.

Targeting MELK prevents Th2 polarization and induces Th1 polarization in cervical tumors

The potential function of MELK in Th1/Th2 polarization was further evaluated by loss-of-function assays. MELK was depleted by shRNAs specifically targeting mouse MELK gene (shMELK-3 and shMELK-4) in U14 cells (Figure 4A). Then, U14 cells transduced with shMELK-3 or shMELK-4 were subcutaneously injected into C57BL/6 mice. In our study, MELK knockdown evidently suppressed the infiltration of Treg, TAM, and MDSCs, and promoted the infiltration of cyto T cells in U14 cervical tumors (Figure 4B). Meanwhile, MELK knockdown repressed the expression of PD-L1, TGFB1, IL-10, and IL-13 in U14 cervical tumors (Figure 4C). The infiltration of Th1 and Th2 cells in U14 cervical tumors was evaluated by flow cytometry. MELK

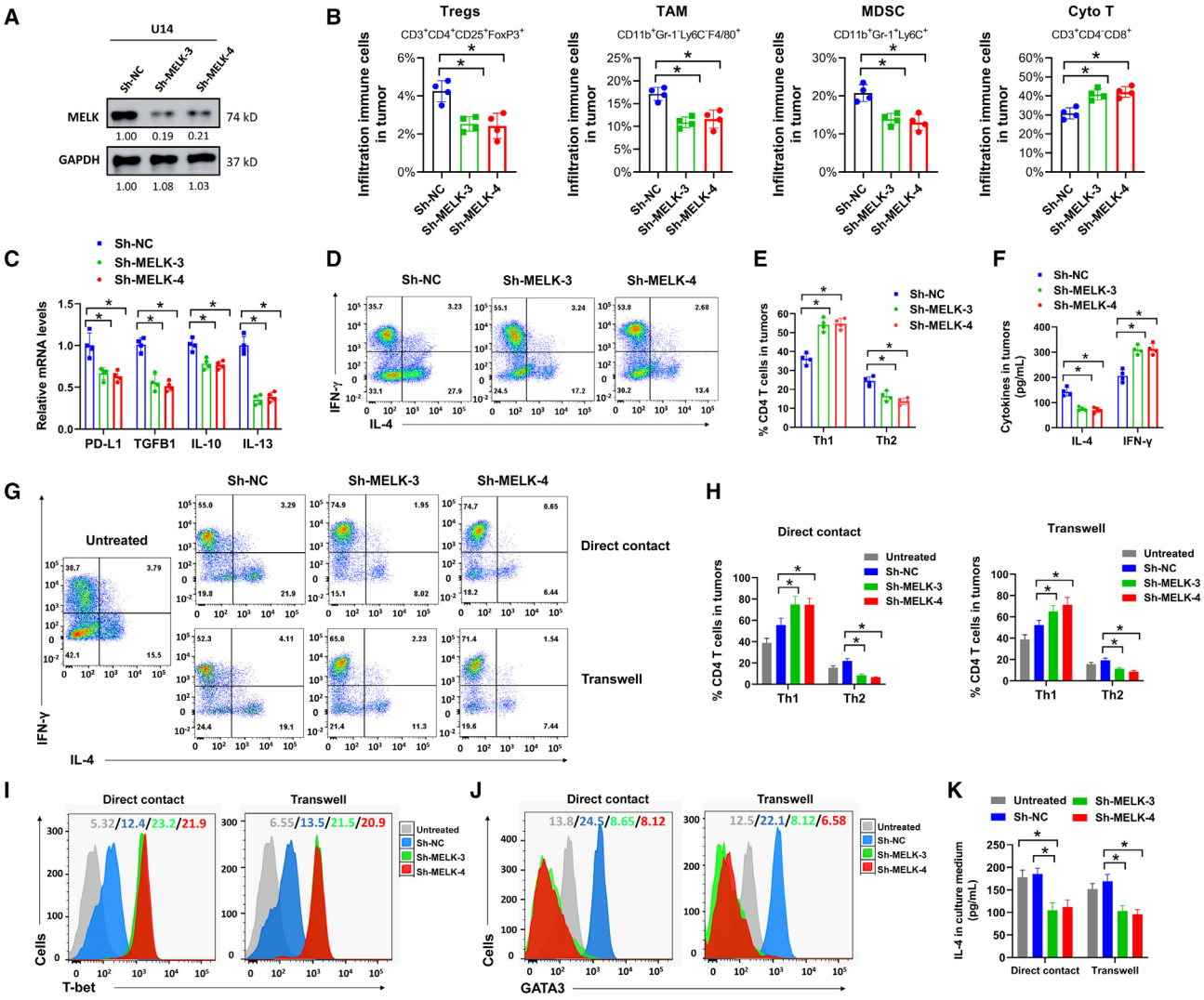

Figure 4. Silencing MELK shifted Th1/Th2 balance toward Th1 bias in mouse cervical tumors

(A) U14 cells were transduced with Sh-NC, shMELK-3, or shMELK-4, and MELK expression was evaluated by western blot. (B) U14 cells (2×10^6) transduced with Sh-NC, shMELK-3, or shMELK-4 were subcutaneously injected into C57BL/6 mice for 4 weeks. Then, infiltrating Treg, TAM, MDSCs, and cyto T cells were evaluated by flow cytometry. (C) Relative expression of PD-L1, TGFB1, IL-10, and IL-13 in Sh-NC, shMELK-3, or shMELK-4 expression U14 tumors were evaluated by quantitative real-time PCR. (D and E) Th1 ($CD3^+CD4^+IFN\text{-}\gamma^+IL4^-$) and Th2 ($CD3^+CD4^+IFN\text{-}\gamma^-IL4^+$) cells in Sh-NC, shMELK-3, or shMELK-4 expression U14 tumors were evaluated by flow cytometry. Representative plots (D) and percentages of Th1 and Th2 cells (E) in $CD4^+$ T cells are shown. (F) IL-4 and IFN-γ production in Sh-NC, shMELK-3, or shMELK-4 expression U14 tumors were evaluated by ELISA. (G–K) Naive T cells isolated from healthy C57BL/6 mice were activated by anti-CD3 and anti-CD28 antibodies, then cocultured with Sh-NC, shMELK-3, or shMELK-4 expression U14 cells by direct contact or indirectly through transwell system. Th1 ($CD3^+CD4^+IFN\text{-}\gamma^+IL4^-$) and Th2 ($CD3^+CD4^+IFN\text{-}\gamma^-IL4^+$) cells were evaluated by flow cytometry. Representative plots (G) and percentages of Th1 and Th2 cells (H) in $CD4^+$ T cells are shown. Representative histogram of T-bet^+ (I) or $GATA3^+$ (J) T cells are shown. IL-4 expression in culture medium was evaluated by ELISA (K). Data are shown as mean ± SD. *$p < 0.05$.

knockdown increased the percentage of Th1 cells and reduced the percentage of Th2 cells in infiltrating $CD4^+$ T cells of U14 cervical tumors (Figures 4D and 4E). MELK knockdown also promoted the production of IFN-γ and suppressed the production of IL-4 in U14 cervical tumors (Figure 4F). Next, the influence of MELK knockdown on Th1 and Th2 polarization was evaluated *in vitro*. Naive T cells isolated from healthy C57BL/6 mice were activated by anti-CD3 and anti-CD28 antibodies, then cocultured with U14 cells by direct contact or indirectly through transwell system. In our study, MELK knockdown in U14 cells evidently promoted Th1 polarization and restrained Th2 polarization of T cells (Figures 4G and 4H). Moreover, the percentage of T-bet^+ T cells was increased, whereas $GATA3^+$ T cells decreased by MELK depletion in U14 cells (Figures 4I and 4J). In addition, MELK knockdown in U14 cells reduced the production of IL-4 by those T cells (Figure 4K). These data indicated that silencing MELK shifted the Th1/Th2 balance toward Th1 bias in

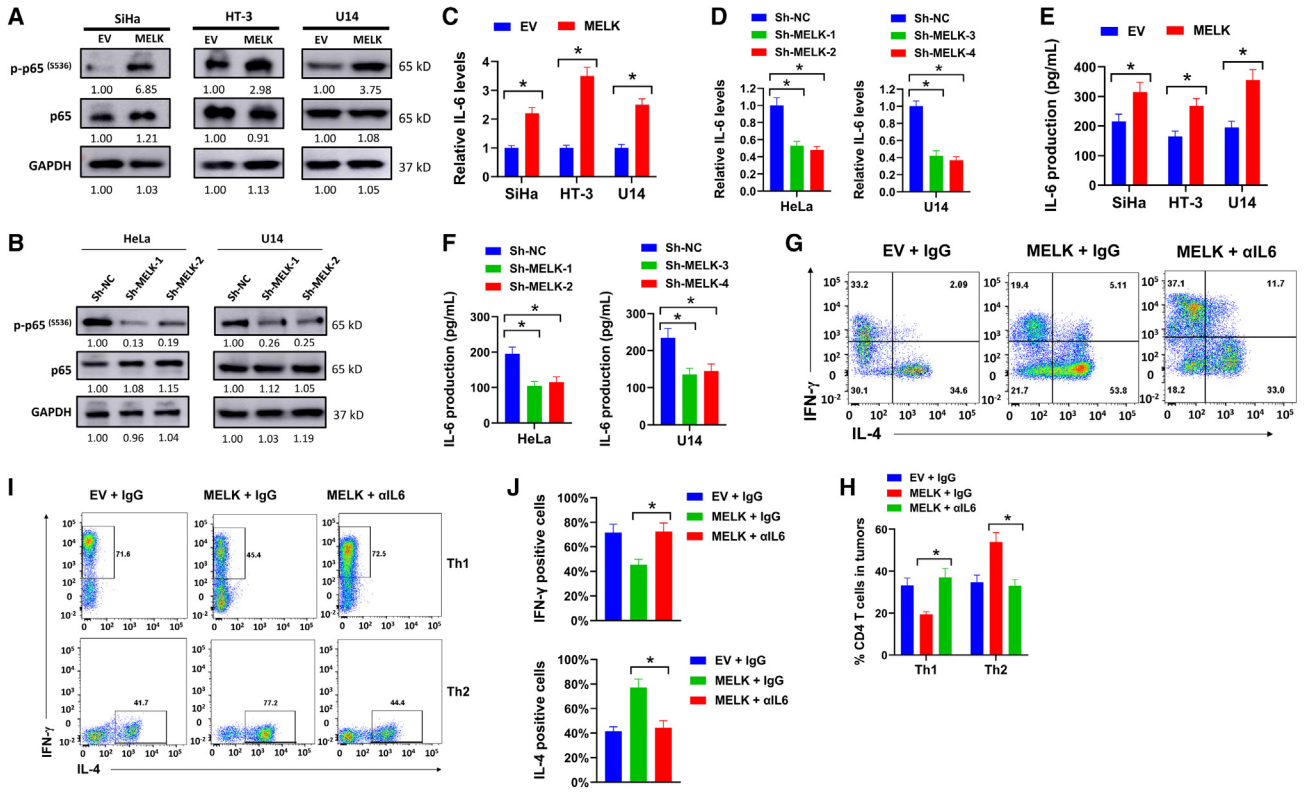

Figure 5. MELK activates NF-κB signaling and promotes IL-6 production by cervical cancer cells

(A) SiHa, HT-3 or U14 cells were transduced with MELK or EV expressing lentivirus, then cell lysates were collected for western blot. (B) HeLa and U14 cells were transduced with Sh-NC, shMELK-1, shMELK-2, shMELK-3, or shMELK-4 expression lentivirus as indicated, then collected lysates for western blot. (C) SiHa, HT-3, and U14 cells were transduced with MELK or EV expressing lentivirus, and relative IL-6 expression was evaluated by quantitative real-time PCR. (D) HeLa and U14 cells were transduced with Sh-NC, shMELK-1, shMELK-2, shMELK-3, or shMELK-4 expression lentivirus as indicated, and relative IL-6 expression was evaluated by quantitative real-time PCR. (E) SiHa, HT-3, and U14 cells were transduced with MELK or EV expressing lentivirus, and IL-6 levels in conditional medium was evaluated by ELISA. (F) HeLa and U14 cells were transduced with Sh-NC, shMELK-1, shMELK-2, shMELK-3, or shMELK-4 expression lentivirus as indicated, and IL-6 levels in conditional medium were evaluated by ELISA. (G and H) U14 cells (2×10^6) transduced with EV or MELK lentivirus were subcutaneously injected into C57BL/6 mice, and received 250 μg antibodies against IL-6 or IgG2b control isotype intraperitoneally every 3 days 7 times to neutralize IL-6 in U14 tumors. Then, Th1 ($CD3^+CD4^+IFN\text{-}\gamma^+IL4^-$) and Th2 ($CD3^+CD4^+IFN\text{-}\gamma^-IL4^+$) cells were evaluated by flow cytometry. Representative plots (G) and percentages of Th1 and Th2 cells (H) in $CD4^+$ T cells are shown. (I and J) Naive T cells from human PBMC were cocultured with EV or MELK transduced SiHa cells indirectly through transwell system under Th1 or Th2 polarizing conditions. Cells were supplemented with 1 μg/mL antibodies against IL-6 or IgG2b control isotype. Representative plots (I) and percentages of $IFN\text{-}\gamma^+IL\text{-}4^-$ Th1 and $IFN\text{-}\gamma^-IL\text{-}4^+$ Th2 cells (J) are shown. Data are shown as mean ± SD. *$p < 0.05$.

mouse cervical tumors *in vitro* and *in vivo*. This was further evaluated in human cells. Naive T cells were isolated from human PBMCs, activated by anti-CD3 and anti-CD28 antibodies, then cocultured with HeLa cells indirectly through transwell system under Th1 or Th2 polarizing conditions. In our study, MELK knockdown in HeLa cells evidently promoted Th1 polarization and suppressed Th2 polarization of human T cells (Figures S6A–S6D). MELK knockdown in HeLa cells also increased the percentage of T-bet$^+$ T cells and decreased the percentage of GATA3$^+$ T cells (Figure S6E). In addition, T cells cocultured with HeLa cells transduced with shMELK-1 or shMELK-2 showed decreased production of IL-4 under Th2 polarizing conditions (Figure S6F). Collectively, these data indicated that targeting MELK prevented Th2 polarization and induced Th1 polarization in cervical tumors.

MELK activates nuclear factor (NF)-κB signaling and promotes IL-6 production by cervical cancer cells

The above results suggested that MELK may modulate the production of some soluble factors by cervical cancer cells. Then, those soluble factors were secreted into the tumor microenvironment and affected the polarization of Th1 and Th2 cells. To test this hypothesis, the potential signaling pathways affected by MELK were evaluated in cervical tumors. Previous studies indicate that MELK regulates the activation of multiple signaling pathways, including NF-κB.[18,19] In our study, MELK overexpression evidently increased the phosphorylation of NF-κB p65 in SiHa, HT-3, and U14 cells, whereas MELK knockdown suppressed the phosphorylation of NF-κB p65 in HeLa and U14 cells, indicating that MELK affected NF-κB activation in cervical cancer cells (Figures 5A and 5B). NF-κB signaling plays an important

role in inflammatory response and tumor development by controlling the production and secretion of various cytokines, such as IL-6.[20] Thus, the secretion of various cytokines was evaluated by ELISA. We found that IL-6 was abundantly produced by SiHa and HT-3 cells and increased by MELK overexpression in cell culture media (Figure S7). Indeed, MELK overexpression increased the mRNA expression of IL-6 in SiHa, HT-3, and U14 cells, whereas MELK knockdown decreased the mRNA expression of IL-6 in HeLa and U14 cells (Figures 5C and 5D). In addition, MELK overexpression apparently promoted the secretion of IL-6 by SiHa, HT-3, and U14 cells (Figure 5E). On the contrary, MELK knockdown suppressed IL-6 secretion by HeLa and U14 cells (Figure 5F). These results indicated that MELK affected IL-6 production and secretion by cervical cancer cells. It is worth noting that IL-6 has been reported to induce Th2 differentiation and suppress Th1 polarization of active $CD4^+$ T cells.[21] Thus, we speculated that MELK affected Th1/Th2 balance by modulating IL-6 secretion by cervical cancer cells. To validate this, neutralizing antibody against IL-6 was used. Our data indicated that the depletion of IL-6 abrogated the influence of MELK overexpression on Th1/Th2 polarization in U14 tumors (Figures 5G and 5H). Moreover, MELK overexpression in SiHa cells promoted Th2 polarization and suppressed Th1 polarization of $CD4^+$ T cells *in vitro*, but this effect was abandoned by the depletion of IL-6 in culture medium (Figures 5I and 5J). Above all, our data indicated that MELK activated NF-κB signaling and promoted IL-6 secretion by cervical cancer cells.

MELK modulates the antitumor activity of cytotoxic $CD8^+$ T cells in cervical tumors

Th1 and Th2 cells are involved in regulating the cytotoxic activity of $CD8^+$ T cells in tumors.[6] In our study, Th2 cells were depleted by IL-4-specific antibody in U14 cervical tumors (Figures S8A and S8B). IFN-γ and tumor necrosis factor-α (TNF-α) are important effectors for the cytotoxic activity of $CD8^+$ T cells. IL-4 neutralization significantly increased the percentage of IFN-γ^+CD8^+ and TNF-α^+CD8^+ T cells in U14 cervical tumors (Figures S8C–S8F). The levels of IFN-γ and TNF-α were also increased by IL-4 neutralization (Figure S8G). Ki67 and granzyme B are markers for the proliferation and activation of $CD8^+$ T cells. IL-4 neutralization increased the percentages of $Ki67^+CD8^+$ or granzyme B^+CD8^+ T cells, indicating increased proliferation and activation of $CD8^+$ T cells (Figure S8H). T cell exhaustion is a state of T cell dysfunction during cancer development. Exhausted $CD8^+$ T cells were marked as PD-1^+Tim-3^+ in our study. We found that the percentage of PD-1^+Tim-3^+ exhausted $CD8^+$ T cells was decreased by IL-4 neutralization in U14 cervical tumors (Figures S8I and S8J). These results indicated that depletion of Th2 cells by IL-4 neutralization enhanced the antitumor activity of cytotoxic $CD8^+$ T cells in cervical tumors. Given that cytotoxic $CD8^+$ T cells play a central role in antitumor immunity, we speculated that MELK may modulate the antitumor activity of $CD8^+$ cytotoxic T cells by affecting Th1/Th2 balance in cervical cancer. In our study, MELK overexpression evidently suppressed the infiltration of cytotoxic $CD8^+$ T cells (Figure 2B), whereas MELK knockdown promoted the infiltration of cytotoxic $CD8^+$ T cells in U14 cervical tumors (Figure 4B). MELK overexpression also reduced the percentage of IFN-γ^+ and TNF-α^+ $CD8^+$ T cells in U14 cervical tumors (Figures 6A–6D). In addition, forced MELK expression reduced the percentages of $Ki67^+$ and granzyme B^+ $CD8^+$ T cells in U14 cervical tumors (Figures 6E and 6F). In addition, MELK overexpression evidently increased the percentage of PD-1^+Tim-3^+ exhausted $CD8^+$ T cells (Figures 6G and 6H). Next, the influence of MELK on the antitumor activity of cytotoxic $CD8^+$ T cells was evaluated by loss-of-function assays. Knockdown of MELK reduced the percentages of IFN-γ^+ and TNF-α^+ $CD8^+$ T cells in U14 cervical tumors (Figures 6I–6L). Moreover, the knockdown of MELK increased the percentages of $Ki67^+$ or granzyme B^+ T cells, indicating increased proliferation and activation of $CD8^+$ T cells (Figure 6M). On the contrary, the percentage of PD-1^+Tim-3^+ exhausted $CD8^+$ T cells was reduced by MELK knockdown (Figures 6N and 6O). These data indicated that MELK modulated the antitumor activity of cytotoxic $CD8^+$ T cells in cervical tumors.

Targeting MELK sensitizes cervical tumors to anti-PD-1 immunotherapy

Because MELK affected Th1/Th2 polarization and activation of cytotoxic $CD8^+$ T cells, we speculated that the efficiency of PD-1 blockade may be influenced by MELK overexpression in cervical tumors. To evaluate this, anti-PD-1 antibody was used in our study. We found that PD-1 blockade significantly suppressed tumor growth of EV-transduced U14 cells, with reduced tumor volume and weight (Figures 7A–7C). However, PD-1 blockade showed no obvious influence on tumor growth of MELK overexpressing U14 cells, indicating that forced MELK expression conferred resistance to PD-1 blockade. The intratumoral infiltrating immune cells were evaluated. PD-1 blockade evidently suppressed the infiltration of Tregs, TAM, MDSCs, and Th2, and promoted the infiltration of cyto T and Th2 cells in EV-transduced U14 tumors compared with immunoglobulin G (IgG) isotype control-treated tumors (Figure 7D). In contrast, PD-1 blockade promoted the infiltration of Th1 cells and restrained the infiltration of Th2, Tregs, and TAM, but showed no influence on the infiltration of cyto T cells and MDSCs in MELK overexpression U14 tumors (Figure 7D). MELK is a member of the AMP-related serine-threonine kinase family. It can be targeted by small inhibitor OTSSP167, which is the only MELK inhibitor that has entered multiple clinical trials.[22] To evaluate the influence of MELK inhibition on PD-1 blockade, OTSSP167 was used in our study. OTSSP167 treatment apparently inhibited MELK expression in U14 tumors (Figure 7E). In addition, OTSSP167 treatment moderately suppressed the tumor growth of IgG-treated U14 tumors compared with vehicle control, with reduced tumor volume and weight (Figures 7F–7H). In contrast, the combination of OTSSP167 and PD-1 treatment dramatically inhibited tumor growth of U14 tumors (Figures 7F–7H). Meanwhile, OTSSP167 treatment enhanced the infiltration of Tregs, TAM, MDSCs, and Th2, and suppressed the infiltration of cyto T and Th2 cells in U14 tumors, and this effect was strengthened by PD-1 blockade (Figures 7F–7H). Above all, our data indicated that targeting MELK sensitized cervical tumors to anti-PD-1 immunotherapy.

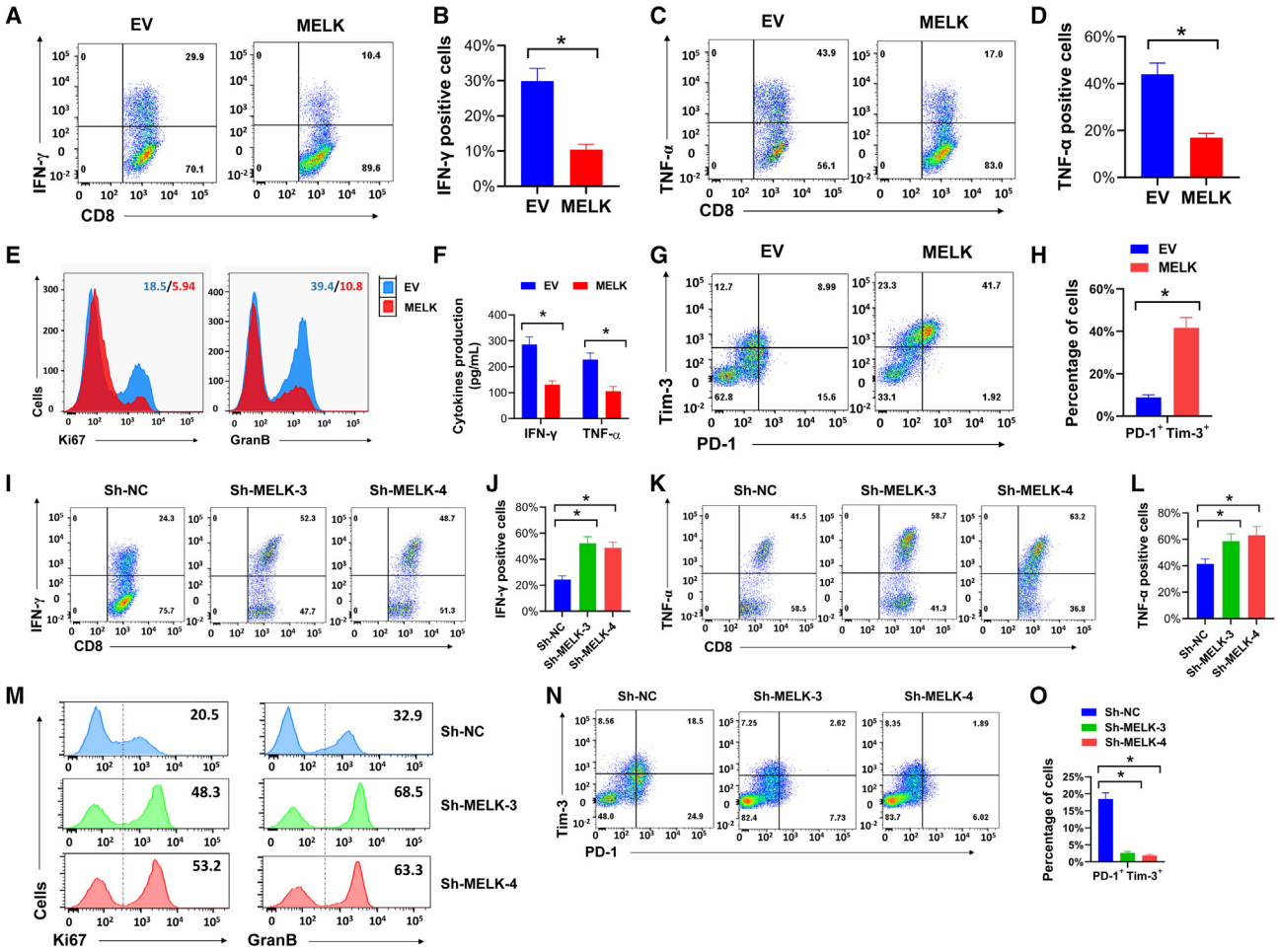

Figure 6. MELK modulates the antitumor activity of cytotoxic CD8$^+$ cells in cervical tumors

(A–H) U14 cells (2 × 10^6) transduced with MELK expression lentivirus or EV control were subcutaneously injected into C57BL/6 mice for 4 weeks. Representative plots (A and C) and percentages of infiltrating IFN-γ$^+$CD8$^+$ and TNF-α$^+$CD8$^+$ T cells are shown (B and D). Representative histogram of Ki67$^+$ and granzyme B$^+$ infiltrating CD8$^+$ T cells are displayed (E). IL-4 and IFN-γ production was evaluated by ELISA (F). Representative plots (G) and percentages of infiltrating PD-1$^+$Tim-3$^+$ CD8$^+$ T cells (H) are shown. (I–O) U14 cells (2 × 10^6) transduced with Sh-NC, shMELK-3, or shMELK-4 were subcutaneously injected into C57BL/6 mice for 4 weeks. Representative plots (I and K) and percentages of infiltrating IFN-γ$^+$CD8$^+$ and TNF-α$^+$CD8$^+$ T cells are shown (J and L). Representative histogram of Ki67$^+$ and granzyme B$^+$ infiltrating CD8$^+$ T cells are displayed (M). Representative plots (N) and percentages of infiltrating PD-1$^+$Tim-3$^+$ CD8$^+$ T cells (O) are shown. Data are shown as mean ± SD. *p < 0.05.

DISCUSSION

Accumulated studies support an oncogenic role for MELK in various cancers, although discrepancies arise from some studies calling into question the essentiality of this kinase in cancer.[23] The major point is that most previous studies evaluated the tumor-promotion role of MELK in cancers by loss-of-function assays using RNAi or pharmacological-mediated MELK inhibition, which raises the question of off-target effects.[23] In addition, recent studies using genetic CRISPR-Cas9-mediated MELK deletion suggest that MELK knockout does not affect the cell proliferation of triple-negative breast cancer cells and other cancer cells.[24] However, it is worth noting that MELK is upregulated in most cancer types, and many studies demonstrate that the antiproliferative effects of RNAi-mediated MELK knockdown can be rescued by restoring MELK expression.[23] In addition, direct evidence proving the oncogenic role of MELK is provided by a recent study in lung cancer.[25] In cervical cancer, two previous studies prove that MELK inhibition by small interfering RNA or small inhibitors suppress growth and induce apoptosis in cervical cancer cells, but lack direct evidence to demonstrate the oncogenic role of MELK.[12,13] In our study, we proved that forced MELK expression promoted cell proliferation, anchorage-dependent growth, and tumor xenograft formation of cervical cancer cells, which further supported the oncogenic role of MELK in cervical cancer.

In the present study, we found that MELK overexpression shifted the Th1/Th2 balance toward Th2 skewed in mouse cervical tumors and active CD4$^+$ T cells from human PBMCs, whereas MELK knockdown showed opposite effects. In fact, high MELK expression

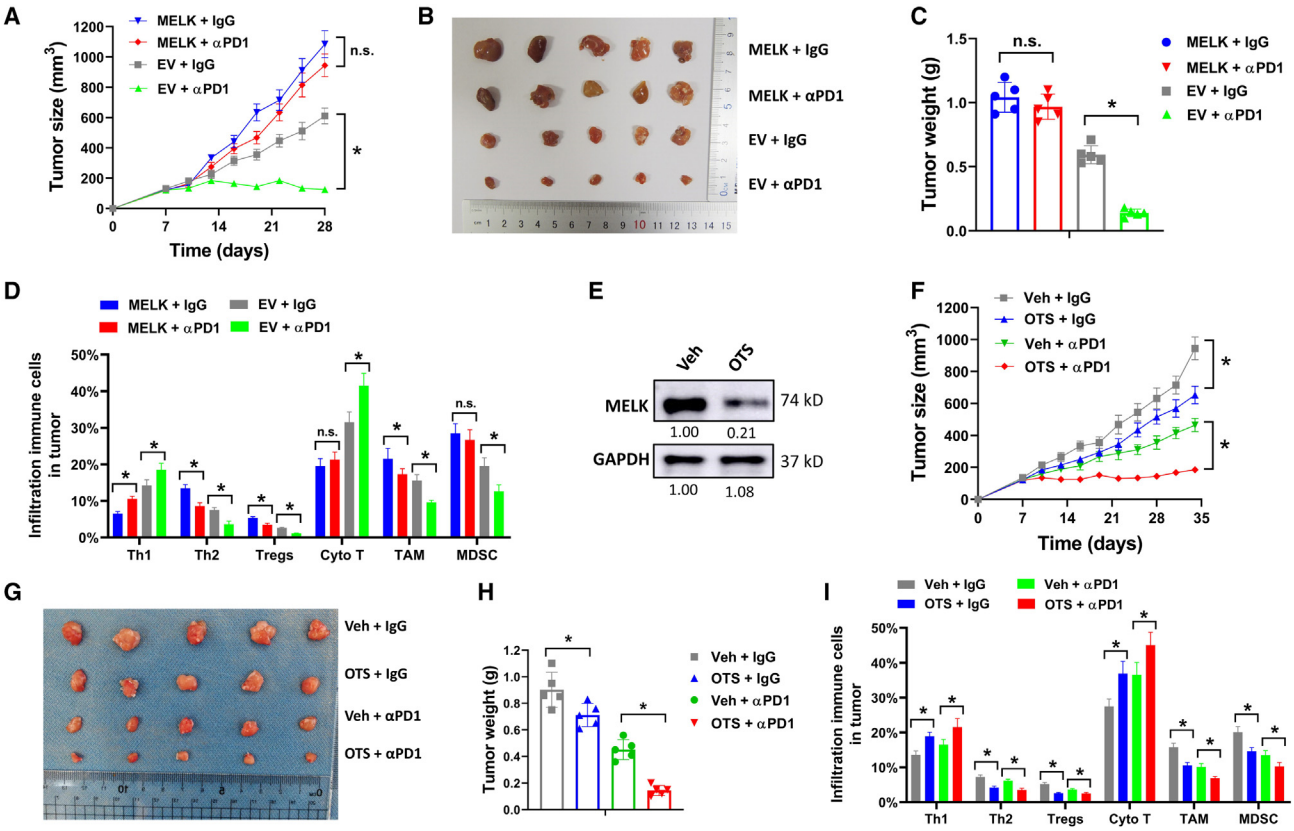

Figure 7. Targeting MELK sensitizes cervical tumors to anti-PD-1 immunotherapy

(A–D) U14 cells (2×10^6) transduced with MELK expression lentivirus or EV control were subcutaneously injected into C57BL/6 mice, then treated with antibodies against PD-1 or IgG2b control isotype intraperitoneally every 3 days 7 times as indicated. Tumor growth curves (A), representative images (B), and tumor weight (C) are shown. Infiltrating immune cells were evaluated by flow cytometry (D). (E–I) U14 cells (2×10^6) were subcutaneously injected into C57BL/6 mice, then treated with 5 mg/kg OTSSP167 (OTS), an equal volume of DMSO (Veh), and antibodies against PD-1 or IgG2b control as indicated. MELK expression was evaluated by western blot (E). Tumor growth curves (F), representative images (G), and tumor weight (H) are displayed. Infiltrating immune cells were evaluated by flow cytometry (I). Data are shown as mean ± SD. *$p < 0.05$.

is positively associated with increasing Th2 infiltration and decreasing Th1 infiltration in most cancer types, as indicated in the TSIDB database. Typically, a shift in favor of Th2 cells results in protumorigenic consequences. For example, a high number of Th2 and Treg cells are found in tumor epithelium, stroma, and peritumoral tertiary lymphoid structures of non-small cell lung cancer samples, whereas Th1 cells are more frequent in noncancerous lung tissue.[26] Meanwhile, a lower ratio of Th1/Th2 is associated with a decreasing number of intratumoral $CD8^+$ T cells in non-small cell lung cancer.[26] Similarly, a profound Th2 bias is found in patients with malignant glioma and metastatic melanoma.[27,28] In myeloma, idiotype protein-specific Th1 and cyto T cells suppress the growth of myeloma cells, whereas Th2 cells promote growth and idiotype protein secretion by myeloma cells, suggesting that Th2 cells have opposite function compared with Th1 and cyto T cells and even promote tumor progression.[29] More important, there is a shift to a Th2-type cytokine pattern in plasma during the progression of cervical cancer, indicating that a favor of Th2 bias during cervical cancer tumorigenesis.[30] We notice that a protumorigenic role of Th2 cells in cancer does not mean that Th2 cells have no anticancer capacity, as reviewed by others.[31] Through the major histocompatibility complex class II pathway, Th2 cells can initiate antitumor responses. However, according to Bretscher's Th2-skewing hypothesis, a weak antitumor immune response sustained by Th2 cells results in tumor escape, and a robust antitumor immune response mediated by Th1 and $CD8^+$ T cells leads to successful antitumor responses.[10,26] This may explain the controversy between the pro- and antitumorigenic roles of Th2 in cancer. In our study, MELK overexpression fostered an immunosuppressive microenvironment in cervical cancer by increasing the intratumoral accumulation of TAM, Treg, and MDSCs and suppressing the infiltration of cyto T cells in mouse cervical tumors. To explain this, we speculated that MELK overexpression promoted Th2 polarization in cervical tumors, which subsequently affected the infiltration of other immune cells. For example, tumor-infiltrating M2 macrophages are induced by Th2-related cytokines such as IL-4, IL-10, and

IL-13.[32–34] Increased Th2 polarization is also associated with elevated MDSC accumulation in cancers.[35,36]

In the present study, MELK activated NF-κB signaling and promoted IL-6 secretion by cervical cancer cells. IL-6 depletion by neutralization antibodies abrogated the influence of MELK overexpression on the polarization of Th1 and Th2 cells in mouse U14 tumors and $CD4^+$ T cells from human PBMCs. Accumulated studies demonstrate that IL-6 promotes Th2 polarization and simultaneously inhibits Th1 polarization of $CD4^+$ T cells.[21] On the one hand, IL-6 promotes Th2 differentiation of naive T cells by upregulating the NF of activated T cells to enhance IL-4 production; on the other hand, IL-6 inhibits Th1 differentiation by upregulating suppressor of cytokine signaling-1 to interfere in IFN-γ signaling.[21,37,38] IL-6 can be produced by antigen-presenting cells and nonimmune cells such as cancer cells.[39] For example, IL-6 produced by tumor cells is modulated by ERK5/MAPK7 signaling, and promotes Th2 differentiation and suppresses Th1 differentiation in lung cancer.[40] In colorectal cancer, MTERFD1 promotes cell growth and irradiation resistance via increasing IL-6 production by colorectal cancer cells.[41] In cervical cancer, the expression level of IL-6 is really high in most cervical cancer cell lines and is measurable in cell supernatant.[42] In our study, MELK overexpression promoted IL-6 production and secretion by cervical cancer cells. There is a feedback loop called IL-6 amplifier (IL-6 Amp).[39] In the IL-6 Amp, IL-6 and NF-κB activators synergistically enhance the production of various proinflammatory cytokines, including IL-6, from nonimmune cells, and promote the recruitment of immune cells into cancer lesions. The interaction between immune cells and nonimmune cells can further strengthen the IL-6 Amp. Thus, we speculated that the influence of MELK overexpression on the polarization of Th1 and Th2 cells may be strengthened by the IL-6 Amp. IL-6 is a multifunctional NF-κB regulated cytokine.[39] In our study, MELK activated NF-κB signaling in cervical cancer cells; thus, we speculated that MELK may support the activation of IL-6 Amp. In fact, there is increasing evidence indicating that MELK regulates NF-κB signaling. MELK kinase is a regulator of EZH2 ubiquitination and turnover.[43,44] MELK phosphorylates EZH2, which subsequently binds and methylates NF-κB to promote its activation.[19] In melanoma, MELK is upregulated by MAPK signaling through the E2F1 transcription factor, and enhances growth of melanoma cells by activating NF-κB signaling.[18]

Priming and expansion of cytotoxic $CD8^+$ T cells demand active help by $CD4^+$ T cells. There is increasing evidence indicating that a shift of Th1/Th2 balance toward a higher ratio of Th2/Th1 limits the antitumor immunity of cytotoxic $CD8^+$ T cells. In brain tumors, tumor-antigen–specific Th1 cells preferentially accumulate in the intracranial tumors compared with Th2 cells, and promote the recruitment and activation of $CD8^+$ T cells in the tumor microenvironment.[45] In breast cancer, Suplatast tosilate IPD-1151 treatment facilitates Th2 to Th1 switching, and enhances the infiltration and cytotoxic activity of $CD8^+$ T cells in tumor tissues.[33] In our study, MELK overexpression shifted Th1/Th2 balance toward Th2 skewed and enhanced the antitumor activity of cytotoxic $CD8^+$ cells in cervical tumors. In recent years, PD-1 blockade has become an alternative choice for cervical cancer treatment. Although the response rate for anti-PD-1 drug pembrolizumab is only ∼15% in cervical patients, it highlights an important first step in using immune checkpoint inhibitors in cervical cancer treatment.[5] In our study, forced MELK expression conferred resistance to PD-1 blockade, whereas depletion of MELK by OTSSP167 significantly enhanced the inhibitory effect of PD-1 blockade in U14 tumors. These results suggested that MELK may be a feasible target to enhance anti-PD-1 immunotherapy in cervical cancer. In addition, MELK is overexpressed and correlated with active $CD4^+$ T, Th1, and Th2 cell infiltration in various cancers, suggesting that these cancers may respond well to the combination treatment with OTSSP167 and anti-PD-1 immunotherapy, but further studies are needed.

Conclusion

We found that MELK was upregulated and played an oncogenic role in cervical cancer. MELK overexpression shifted Th1/Th2 balance toward Th2 skewed, whereas knockdown of MELK showed opposite effects. MELK activated NF-κB signaling and promoted IL-6 secretion by cervical cancer cells. In addition, MELK modulated the antitumor activity of cytotoxic $CD8^+$ cells in cervical tumors. MELK overexpression conferred resistance to PD-1 blockade, and depletion of MELK by OTSSP167 significantly enhanced the inhibitory effect of PD-1 blockade in U14 tumors. Our results provided a novel role for MELK in regulating Th1/Th2 balance and anti-PD-1 immunotherapy in cervical cancer.

MATERIALS AND METHODS

Cell culture

Human cervical cell lines SiHa, HT-3, HeLa, Ca Ski, and C-33A and the mouse U14 cervical cancer cell line were obtained from the Institute of Biochemistry and Cell Biology at the Chinese Academy of Sciences (Shanghai, China). Ca Ski was maintained in RPMI 1640 (Hyclone, USA). SiHa, HT-3, HeLa, C-33A, and U14 were maintained in DMEM (Hyclone). All of the cells were cultured with 10% fetal bovine serum (FBS, Gibco, USA) and 1% streptomycin and penicillin in a humidified atmosphere at 37°C containing 5% CO_2.

T cell polarization

The collection and use of human samples were approved by the Ethics Committee of The First Hospital of Jilin University. Written informed consent was obtained from all of the enrolled subjects. Blood samples from healthy donors were collected, and PBMCs were isolated by Ficoll reagents (Sigma, USA) according to the manufacturers' instruction. Naive T cells ($CD62L^{hi}CD44^{lo}$) were sorted and used for T cell polarization assays from human PBMCs. To evaluate the influence of U14 cells on T cell polarization, naive T cells were cocultured with U14 cells by direct contact or transwell chamber in the presence of anti-CD3 (2 μg/mL), anti-CD28 (2 μg/mL), and IL-2 (20 ng/mL) for 5 days. To evaluate the influence of SiHa, HT-3, and HeLa cells on Th1 polarization, naive T cells were cocultured with SiHa, HT-3, or HeLa cells indirectly by transwell chamber in the presence of anti-CD3 (2 μg/mL), anti-CD28 (2 μg/mL), IL-2 (20 ng/mL),

anti-IL-4 (10 μg/mL), and IL-12 (20 ng/mL) for 5 days. To evaluate the influence of SiHa, HT-3, and HeLa cells on Th2 polarization, naive T cells were cocultured with SiHa, HT-3, or HeLa cells indirectly by transwell chamber in the presence of anti-CD3 (2 μg/mL), anti-CD28 (2 μg/mL), anti-IFN-γ (10 μg/mL), and IL-4 (20 ng/mL) for 5 days.

Plasmid constructs

MELK expression lentivirus vector was constructed by inserting human or mouse MELK coding sequence into the pCDH vector (System Biosciences no. CD510B, USA). EV was regarded as control. MELK knockdown lentivirus vectors were constructed by inserting shRNAs targeting human MELK (shMELK-1 and shMELK-2) or mouse MELK (shMELK-3 and shMELK-4) into the pLKO.1 vector. The pLKo.1 vector inserted with a nontargeting sequence was used as control (Sh-NC). The sequences were shMELK-1, 5′-CTCTT AACTA TGTCT CTTTGT-3′; shMELK-2, 5′-GCCTG AAAGA AACTC CAATTA-3′; shMELK-3, 5′-GCCTG GGTTT ACAAG AGATTA-3′; shMELK-4, 5′-GCTGG ATTGAT AGAC TATGAA-3′; and Sh-NC, 5′-ACGGA GGCTA AGCGT CGCAA-3′.

Cell viability assay

Cell Counting Kit-8 (CCK-8, Takara, Japan) was used to evaluate the viability of cells. In brief, SiHa, HT-3, or HeLa cells were seeded in 96-well plates (3,000/well), and cell viability was evaluated at days 0, 2, 4, and 6. CCK-8 solution (10 μL/well) was added to each well at indicated time points and incubated for 2 h at 37°C. Then, the absorbance at 450 nm was measured by a microplate reader. Each sample had three repeats.

Soft agar assay

Soft agar assay was conducted as previously described.[46] Briefly, the 6-well plates were layered with 0.6% bottom agar, and cells (5,000/well) were seeded in 0.4% top agar. The bottom and top agars containing RPMI 1640 medium were supplemented with 10% FBS and 1% streptomycin and penicillin. Cells were cultured for 2 weeks, and colonies were imaged by a microscope. Each sample had three duplicates.

Quantitative real-time PCR

Total RNAs were extracted using TRIzol reagent (Takara, Japan) and reverse transcribed into cDNAs using Superscript III first-strand synthesis kit (Invitrogen, USA). SYBR Green/ROX PCR master mix (Invitrogen, USA) was used for quantitative real-time PCR on the ABI 7900HT qPCR system (ABI Biosystems, USA). Relative gene expression was normalized to glyceraldehyde 3-phosphate dehydrogenase (GAPDH) and calculated by the $2^{-\Delta\Delta Cq}$ method. Primers are listed in Table S1.

Western blot

Protein lysates were extracted by radioimmunoprecipitation assay lysis buffer (Beyotime, China) supplemented with protease inhibitor cocktail (Sigma, USA). A total of 20 μg protein lysates were separated by 10% SDS-PAGE and transferred to polyvinylidene fluoride membranes (Millipore, USA). Next, membranes were blocked by 5% nonfat milk, then incubated with primary antibodies at 4°C on a rotator overnight and secondary antibodies at room temperature for 1 h. Western blot bands were detected by the ECL kit (Thermo Fisher Scientific, USA). The antibodies were as follows: MELK antibody (Abcam, no. ab273015, UK), GAPDH (Abcam, no. ab8245), NF-κB p65 (Cell Signaling Technology, no. 8242, USA), and phospho-NF-κB $p65^{Ser536}$ (Cell Signaling Technology, no. 3033).

Flow cytometry

Tumor xenografts were cut into pieces and digested with collagenase IV (Sigma, USA) and DNAse I (Sigma, USA) for 30 min at 37°C. Then, cell suspensions were passed through a 70-μm strainer to remove undigested tissues. Erythrocytes were removed by Red Blood Cell Lysis Solution (Qiagen, USA). For cell surface staining, 1×10^6 cells were incubated with anti-Fc receptor blocking antibody at 4°C for 30 min. For intracellular staining, 1×10^6 cells were fixed and permeabilized using the Fixation/Permeabilization Solution Kit (BD Bioscience, USA) according to the manufacturer's instructions. Then, cells were stained with the indicated antibodies for 30 min at 4°C. Flow cytometry was performed using a BD Influx cell sorter (BD Bioscience). Flow cytometry data were analyzed by FlowJo version 10 (FlowJo, USA). The flow cytometry antibodies used in our study were CD45 APC, CD4 PE, CD8a V450, CD25 APC-CY7, FoxP3 PE-CY7, IFN-γ PE-CY7, IL-4 APC-CY7, Gr-1 V450, Ly6C FITC, CD11 b PE, F4/80 APC-CY7, Tim-3 PE-CY7, PD-1 PerCP CY5.5, T-bet FITC, GATA3 APC, TNF-α APC-CY7, anti-Ki67 FITC, and anti-Granzyme B PE, all from BD Bioscience.

Bioinformatic analysis

Data of TCGA cervical cancer subset were downloaded from the GDC Data Portal (https://gdac.broadinstitute.org/). GEO datasets (GSE 6791, GSE52903, and GSE67522) were assessed from https://www.ncbi.nlm.nih.gov/geo/. MELK expressions in those datasets were re-analyzed by us to evaluate the expression of MELK in cervical cancer patients. TIMER (https://cistrome.shinyapps.io/timer/) and TISIDB (http://cis.hku.hk/TISIDB/) were used to evaluate the correlation of MELK expressions with tumor-infiltrating immune cells and immune modulators in the cervical cancer dataset.

ELISA assay

The levels of IL-1α, IL-1β, IL-6, IL-8, IL-10, granulocyte macrophage-colony-stimulating factor (GM-CSF), G-CSF, TNF-α, monocyte chemoattractant protein-1, macrophage inflammatory protein-1α, IL-4, and IFN-γ were evaluated by ELISA assay kits (Abcam) as protocol described. In brief, serum samples or conditional medium were incubated with antibody-coated plates for 1 h at room temperature, then washed with PBS 5 times. Next, biotinylated antibodies, streptavidin antibodies, substrate solution, and stop solution were used consecutively as protocol indicated. Finally, the absorbance at 450 nm was measured for each well. Each sample had three repeats.

Murine cervical cancer models

Animal studies were reviewed and approved by the Institutional Animal Care and Use Committee of The First Hospital of Jilin University (Approval no: 2022-0486). SiHa cells (2×10^6) transduced with EV or MELK lentivirus, or HeLa cells (2×10^6) transduced with Sh-NC, shMELK-1, or shMELK-2 lentivirus were subcutaneously injected into 6-week-old female BALB/c nude mice (n = 5 for each group). Tumor xenografts were allowed to grow for 3 weeks. Tumor volume was measured every 3 days by the formula (length × width2)/2. At the end of the experiment, mice were anesthetized by 3% isoflurane and sacrificed by cervical dislocation. Tumors were dissected out and weighed. To evaluate the influence of MELK on the cervical cancer microenvironment, U14 cells (2×10^6) transduced with EV, MELK, Sh-NC, shMELK-1, or shMELK-2 lentivirus were subcutaneously injected into 6-week-old female C57BL/6 mice. Mice were sacrificed 4 weeks posttumor implantation, and infiltrating immune cells were evaluated by flow cytometry. In separate experiments, U14 cells (2×10^6) transduced with EV or MELK were subcutaneously injected into 6-week-old female C57BL/6 mice. One week later, mice were treated with 250 μg antibodies against IL-4, IL-6, or PD-1 (BioXCell, USA) or IgG2b control isotype intraperitoneally every 3 days 7 times to neutralize IL-4, IL-6, or PD-1 in U14 tumors. OTSSP167 (5 mg/kg; Selleck no. S7159, USA) was treated intraperitoneally every 3 days for 7 days to deplete MELK expression in U14 tumors, and an equal volume of DMSO was used as vehicle control.

Statistical analysis

Data were analyzed by GraphPad Prism 9 (GraphPad Software, USA). The results were presented as means ± SDs. Differences between groups were analyzed by two-tailed Student's t test and one-way ANOVA (Bonferroni's post hoc test). Data with $p < 0.05$ were considered statistically significant.

DATA AND CODE AVAILABILITY

The data that support the findings of this study are available on request from the corresponding author.

SUPPLEMENTAL INFORMATION

Supplemental information can be found online at https://doi.org/10.1016/j.omton.2024.200759.

ACKNOWLEDGMENTS

This study was supported by the Jilin Tianhua Health Charity Foundation (Z2022LJL001) and the China Zhongguancun Precision Medicine Science and Technology Foundation (JZYX7799). The experiments involving human subjects were followed with the ethical standards of the institutional committee of The First Hospital of Jilin University and with the 1964 Declaration of Helsinki and its later amendments or comparable ethical standards. The animal studies were followed with the ethical standards of the ethics committee of The First Hospital of Jilin University.

AUTHOR CONTRIBUTIONS

All of the authors guaranteed the integrity of the entire study. The experiments were conducted by D.W., F.Z., and Y.L. The clinical studies were conducted by J.H. Data were analyzed by D.W. The manuscript was prepared and reviewed by L.G. All of the authors have read and approved the manuscript.

DECLARATION OF INTERESTS

The authors declare no competing interests.

REFERENCES

1. Sung, H., Ferlay, J., Siegel, R.L., Laversanne, M., Soerjomataram, I., Jemal, A., and Bray, F. (2021). Global Cancer Statistics 2020: GLOBOCAN Estimates of Incidence and Mortality Worldwide for 36 Cancers in 185 Countries. CA A Cancer J. Clin. *71*, 209–249.
2. Hu, Z., and Ma, D. (2018). The precision prevention and therapy of HPV-related cervical cancer: new concepts and clinical implications. Cancer Med. *7*, 5217–5236.
3. Turinetto, M., Valsecchi, A.A., Tuninetti, V., Scotto, G., Borella, F., and Valabrega, G. (2022). Immunotherapy for Cervical Cancer: Are We Ready for Prime Time? Int. J. Mol. Sci. *23*, 3559.
4. Enwere, E.K., Kornaga, E.N., Dean, M., Koulis, T.A., Phan, T., Kalantarian, M., Köbel, M., Ghatage, P., Magliocco, A.M., Lees-Miller, S.P., and Doll, C.M. (2017). Expression of PD-L1 and presence of CD8-positive T cells in pre-treatment specimens of locally advanced cervical cancer. Mod. Pathol. *30*, 577–586.
5. Chung, H.C., Ros, W., Delord, J.P., Perets, R., Italiano, A., Shapira-Frommer, R., Manzuk, L., Piha-Paul, S.A., Xu, L., Zeigenfuss, S., et al. (2019). Efficacy and Safety of Pembrolizumab in Previously Treated Advanced Cervical Cancer: Results From the Phase II KEYNOTE-158 Study. J. Clin. Oncol. *37*, 1470–1478.
6. Basu, A., Ramamoorthi, G., Albert, G., Gallen, C., Beyer, A., Snyder, C., Koski, G., Disis, M.L., Czerniecki, B.J., and Kodumudi, K. (2021). Differentiation and Regulation of T(H) Cells: A Balancing Act for Cancer Immunotherapy. Front. Immunol. *12*, 669474.
7. Zhu, J. (2018). T Helper Cell Differentiation, Heterogeneity, and Plasticity. Cold Spring Harbor Perspect. Biol. *10*, a030338.
8. Corthay, A., Skovseth, D.K., Lundin, K.U., Røsjø, E., Omholt, H., Hofgaard, P.O., Haraldsen, G., and Bogen, B. (2005). Primary antitumor immune response mediated by CD4+ T cells. Immunity *22*, 371–383.
9. Qin, Z., and Blankenstein, T. (2000). CD4+ T cell–mediated tumor rejection involves inhibition of angiogenesis that is dependent on IFN gamma receptor expression by nonhematopoietic cells. Immunity *12*, 677–686.
10. Bretscher, P. (2019). On Analyzing How the Th1/Th2 Phenotype of an Immune Response Is Determined: Classical Observations Must Not Be Ignored. Front. Immunol. *10*, 1234.
11. Jiang, P., and Zhang, D. (2013). Maternal embryonic leucine zipper kinase (MELK): a novel regulator in cell cycle control, embryonic development, and cancer. Int. J. Mol. Sci. *14*, 21551–21560.
12. Sun, H., Ma, H., Zhang, H., and Ji, M. (2021). Up-regulation of MELK by E2F1 promotes the proliferation in cervical cancer cells. Int. J. Biol. Sci. *17*, 3875–3888.
13. Wang, J., Wang, Y., Shen, F., Xu, Y., Zhang, Y., Zou, X., Zhou, J., and Chen, Y. (2018). Maternal embryonic leucine zipper kinase: A novel biomarker and a potential therapeutic target of cervical cancer. Cancer Med. *7*, 5665–5678.
14. Liu, Y., Li, R., Wang, X., Xue, Z., Yang, X., and Tang, B. (2022). Comprehensive Analyses of MELK-Associated ceRNA Networks Reveal a Potential Biomarker for Predicting Poor Prognosis and Immunotherapy Efficacy in Hepatocellular Carcinoma. Front. Cell Dev. Biol. *10*, 824938.
15. Oshi, M., Gandhi, S., Huyser, M.R., Tokumaru, Y., Yan, L., Yamada, A., Matsuyama, R., Endo, I., and Takabe, K. (2021). MELK expression in breast cancer is associated with infiltration of immune cell and pathological compete response (pCR) after neoadjuvant chemotherapy. Am. J. Cancer Res. *11*, 4421–4437.

16. Yang, H., Zhou, H., Wang, G., Tian, L., Li, H., Zhang, Y., and Xue, X. (2022). MELK is a prognostic biomarker and correlated with immune infiltration in glioma. Front. Neurol. *13*, 977180.

17. Grivennikov, S.I., Greten, F.R., and Karin, M. (2010). Immunity, inflammation, and cancer. Cell *140*, 883–899.

18. Janostiak, R., Rauniyar, N., Lam, T.T., Ou, J., Zhu, L.J., Green, M.R., and Wajapeyee, N. (2017). MELK Promotes Melanoma Growth by Stimulating the NF-kappaB Pathway. Cell Rep. *21*, 2829–2841.

19. Liu, H., Sun, Y., Qi, X., Gordon, R.E., O'Brien, J.A., Yuan, H., Zhang, J., Wang, Z., Zhang, M., Song, Y., et al. (2019). EZH2 Phosphorylation Promotes Self-Renewal of Glioma Stem-Like Cells Through NF-kappaB Methylation. Front. Oncol. *9*, 641.

20. He, G., and Karin, M. (2011). NF-kappaB and STAT3 - key players in liver inflammation and cancer. Cell Res. *21*, 159–168.

21. Diehl, S., and Rincón, M. (2002). The two faces of IL-6 on Th1/Th2 differentiation. Mol. Immunol. *39*, 531–536.

22. Ren, L., Guo, J.S., Li, Y.H., Dong, G., and Li, X.Y. (2022). Structural classification of MELK inhibitors and prospects for the treatment of tumor resistance: A review. Biomed. Pharm. *156*, 113965.

23. McDonald, I.M., and Graves, L.M. (2020). Enigmatic MELK: The controversy surrounding its complex role in cancer. J. Biol. Chem. *295*, 8195–8203.

24. Lin, A., Giuliano, C.J., Sayles, N.M., and Sheltzer, J.M. (2017). CRISPR/Cas9 mutagenesis invalidates a putative cancer dependency targeted in on-going clinical trials. Elife *6*, e24179.

25. Tang, Q., Li, W., Zheng, X., Ren, L., Liu, J., Li, S., Wang, J., and Du, G. (2020). MELK is an oncogenic kinase essential for metastasis, mitotic progression, and programmed death in lung carcinoma. Signal Transduct. Targeted Ther. *5*, 279.

26. Frafjord, A., Buer, L., Hammarström, C., Aamodt, H., Woldbæk, P.R., Brustugun, O.T., Helland, Å., Øynebråten, I., and Corthay, A. (2021). The Immune Landscape of Human Primary Lung Tumors Is Th2 Skewed. Front. Immunol. *12*, 764596.

27. Shimato, S., Maier, L.M., Maier, R., Bruce, J.N., Anderson, R.C.E., and Anderson, D.E. (2012). Profound tumor-specific Th2 bias in patients with malignant glioma. BMC Cancer *12*, 561.

28. Nevala, W.K., Vachon, C.M., Leontovich, A.A., Scott, C.G., Thompson, M.A., and Markovic, S.N.; Melanoma Study Group of the Mayo Clinic Cancer Center (2009). Evidence of systemic Th2-driven chronic inflammation in patients with metastatic melanoma. Clin. Cancer Res. *15*, 1931–1939.

29. Hong, S., Qian, J., Yang, J., Li, H., Kwak, L.W., and Yi, Q. (2008). Roles of idiotype-specific t cells in myeloma cell growth and survival: Th1 and CTL cells are tumoricidal while Th2 cells promote tumor growth. Cancer Res. *68*, 8456–8464.

30. Bais, A.G., Beckmann, I., Lindemans, J., Ewing, P.C., Meijer, C.J.L.M., Snijders, P.J.F., and Helmerhorst, T.J.M. (2005). A shift to a peripheral Th2-type cytokine pattern during the carcinogenesis of cervical cancer becomes manifest in CIN III lesions. J. Clin. Pathol. *58*, 1096–1100.

31. Schreiber, S., Hammers, C.M., Kaasch, A.J., Schraven, B., Dudeck, A., and Kahlfuss, S. (2021). Metabolic Interdependency of Th2 Cell-Mediated Type 2 Immunity and the Tumor Microenvironment. Front. Immunol. *12*, 632581.

32. Jenkins, S.J., Ruckerl, D., Cook, P.C., Jones, L.H., Finkelman, F.D., van Rooijen, N., MacDonald, A.S., and Allen, J.E. (2011). Local macrophage proliferation, rather than recruitment from the blood, is a signature of TH2 inflammation. Science *332*, 1284–1288.

33. Chen, Y., Sun, J., Luo, Y., Liu, J., Wang, X., Feng, R., Huang, J., Du, H., Li, Q., Tan, J., et al. (2022). Pharmaceutical targeting Th2-mediated immunity enhances immunotherapy response in breast cancer. J. Transl. Med. *20*, 615.

34. Espinosa Gonzalez, M., Volk-Draper, L., Bhattarai, N., Wilber, A., and Ran, S. (2022). Th2 Cytokines IL-4, IL-13, and IL-10 Promote Differentiation of Pro-Lymphatic Progenitors Derived from Bone Marrow Myeloid Precursors. Stem Cell. Dev. *31*, 322–333.

35. Neri, D., Carevic-Neri, M., Brück, J., Holstein, J., Schäfer, I., Solimani, F., Handgretinger, R., Hartl, D., and Ghoreschi, K. (2021). Arginase 1(+) IL-10(+) polymorphonuclear myeloid-derived suppressor cells are elevated in patients with active pemphigus and correlate with an increased Th2/Th1 response. Exp. Dermatol. *30*, 782–791.

36. Gabitass, R.F., Annels, N.E., Stocken, D.D., Pandha, H.A., and Middleton, G.W. (2011). Elevated myeloid-derived suppressor cells in pancreatic, esophageal and gastric cancer are an independent prognostic factor and are associated with significant elevation of the Th2 cytokine interleukin-13. Cancer Immunol. Immunother. *60*, 1419–1430.

37. Diehl, S., Anguita, J., Hoffmeyer, A., Zapton, T., Ihle, J.N., Fikrig, E., and Rincón, M. (2000). Inhibition of Th1 differentiation by IL-6 is mediated by SOCS1. Immunity *13*, 805–815.

38. Rincón, M., Anguita, J., Nakamura, T., Fikrig, E., and Flavell, R.A. (1997). Interleukin (IL)-6 directs the differentiation of IL-4-producing CD4+ T cells. J. Exp. Med. *185*, 461–469.

39. Hirano, T. (2021). IL-6 in inflammation, autoimmunity and cancer. Int. Immunol. *33*, 127–148.

40. Riegel, K., Yurugi, H., Schlöder, J., Jonuleit, H., Kaulich, M., Kirschner, F., Arnold-Schild, D., Tenzer, S., Schild, H., and Rajalingam, K. (2021). ERK5 modulates IL-6 secretion and contributes to tumor-induced immune suppression. Cell Death Dis. *12*, 969.

41. Liu, X., Cao, X., Liu, C., Cao, Y., Zhao, Q., Tan, X., Li, X., Xu, X., Yu, E., and Wang, H. (2019). MTERFD1 promotes cell growth and irradiation resistance in colorectal cancer by upregulating interleukin-6 and interleukin-11. Int. J. Biol. Sci. *15*, 2750–2762.

42. Otani, S., Fujii, T., Kukimoto, I., Yamamoto, N., Tsukamoto, T., Ichikawa, R., Nishio, E., and Iwata, A. (2019). Cytokine expression profiles in cervical mucus from patients with cervical cancer and its precursor lesions. Cytokine *120*, 210–219.

43. Liu, H., Sun, Q., Sun, Y., Zhang, J., Yuan, H., Pang, S., Qi, X., Wang, H., Zhang, M., Zhang, H., et al. (2017). MELK and EZH2 Cooperate to Regulate Medulloblastoma Cancer Stem-like Cell Proliferation and Differentiation. Mol. Cancer Res. *15*, 1275–1286.

44. Li, B., Yan, J., Phyu, T., Fan, S., Chung, T.H., Mustafa, N., Lin, B., Wang, L., Eichhorn, P.J.A., Goh, B.C., et al. (2019). MELK mediates the stability of EZH2 through site-specific phosphorylation in extranodal natural killer/T-cell lymphoma. Blood *134*, 2046–2058.

45. Hoepner, S., Loh, J.M.S., Riccadonna, C., Derouazi, M., Maroun, C.Y., Dietrich, P.Y., and Walker, P.R. (2013). Synergy between CD8 T cells and Th1 or Th2 polarised CD4 T cells for adoptive immunotherapy of brain tumours. PLoS One *8*, e63933.

46. Li, Z., Shao, C., Liu, X., Lu, X., Jia, X., Zheng, X., Wang, S., Zhu, L., Li, K., Pang, Y., et al. (2020). Oncogenic ERBB2 aberrations and KRAS mutations cooperate to promote pancreatic ductal adenocarcinoma progression. Carcinogenesis *41*, 44–55.